32ND INTERNATIONAL COSMIC RAY CONFERENCE, BEIJING 2011

Expected Gamma-Ray Emission of Supernova Remnant SN 1987A

E.G. BEREZHKO[1], L.T. KSENOFONTOV[1], H.J. VÖLK[2]
[1] *Yu.G. Shafer Institute of Cosmophysical Research and Aeronomy, 31 Lenin Avenue, 677980 Yakutsk, Russia*
[2] *Max-Planck-Institute for Nuclear Physiscs, P.O. Box 103980, D-69029 Heidelberg*
Heinrich.Voelk@mpi-hd.mpg.de
DOI: 10.7529/ICRC2011/V08/0106

Abstract: A nonlinear kinetic theory of cosmic ray (CR) acceleration in supernova remnants (SNRs) is employed to re-examine the nonthermal properties of the remnant of SN 1987A for an extended evolutionary period of 5-100 yr. It is shown that efficient production of nuclear CRs leads to a strong modification of the outer SNR shock and to a large downstream magnetic field $B_{\rm d} \approx 20$ mG. The shock modification and the strong field are required to yield the steep and concave radio emission spectrum observed, as well as to considerable synchrotron cooling of high energy electrons which diminishes their X-ray synchrotron flux. These features are also consistent with the existing X-ray observations. The expected gamma-ray energy flux at TeV-energies at the current epoch is nearly $\epsilon_\gamma F_\gamma \approx 4 \times 10^{-13}$ erg cm^{2}s^{-1} under reasonable assumptions about the overall magnetic field topology and the turbulent perturbations of this field. The general nonthermal strength of the source is expected to increase roughly by a factor of two over the next 15 to 20 yrs, before the source will go into a steady emission decrease as the supernova remnant (SNR) shock leaves the immediate circumstellar environment and propagates secularly into the progenitor star's unperturbed Red Supergiant (RSG) wind region.

Keywords: acceleration of particles — gamma rays: general — ISM: individual objects (SN 1987A) — ISM: supernova remnants — X-rays: individual (SN 1987A).

1 Introduction

The Supernova (SN) which occurred in 1987 in the nearby Large Magellanic Cloud was the first object of its kind in modern times whose evolution could be spatially resolved as a function of time; this includes the characterization of the rather massive progenitor star. SN 1987A has been extensively studied in all wavelengths from the radio to the gamma-ray range. For a summary of its global characteristics, see e.g. [1]. The present work concentrates on the nonthermal characteristics and, in particular, on the particle acceleration aspects and the expected gamma-ray emission (for a detailed account, see [2]). It extends two earlier studies [3,4] to include the subsequent *Chandra* observations of the soft and hard X-ray emission [5], as well as the most recent and very detailed observations of the radio continuum (synchrotron) emission [6]. At the same time a qualitative and in fact semi-quantitative prediction of the future nonthermal emission from this source for the next decades is attempted.

The radio synchrotron emission is important for the determination of the total nonthermal energy density in the source. The softness of the observed spectrum shows that the radio electrons are accelerated in a rather weak shock. This is the plasma subshock formed when the accelerated nuclei modify the SNR blast wave by their pressure gradient, so that the main gas compression occurs in an extended CR precursor that does not accelerate radio electrons. This nonlinear modification is used to determine the injection rate of the accelerating nuclear particles and vize versa in a semi-empirical way. It therefore allows a *prediction* of the hadronic gamma-ray emission strength, given also the gas dynamic parameters of the system, like gas density, shock radius and shock velocity (see figure 1). The new *Chandra* data in addition suggest that the hard X-ray emission is predominantly nonthermal. Since at the corresponding electron energies synchrotron losses are of overriding importance for the shaping of the X-ray synchrotron spectrum, these new observations also determine the effective magnetic field strength in the source (for a review, see [7]).

The observed shape of the remnant, especially at radio frequencies, is not very far from spherically symmetric, even though the observed emission varies around the remnant's periphery [8]. This suggests that a spherically symmetric model is a reasonable first order approximation for a study of the general nonthermal properties of the remnant.

2 Theoretical model

Assuming that the progenitor star has gone through three successive wind phases, the innermost region contains the tenuous free wind of the blue supergiant (BSG) progenitor star. This wind terminates in a shock. The subsequent wind bubble sweeps up the slow wind material of the previ-

ous red supergiant (RSG) precursor phase into a very much denser H II region [9], photoionized by the central progenitor star, followed by a neutral, dense, ring-like structure that has its highest density near the equator. This is called the equatorial ring. The ring is nevertheless approximated here by a spherically symmetric shell at a radial distance $R_{\rm R} = 7 \times 10^{17}$ cm. Beyond is freely coasting RSG wind and, even further out, the initial main sequence wind region that is of no concern here. At the present time the SNR shock has already entered the equatorial ring. The shell parameters chosen are consistent with canonical values of stellar ejecta mass $M_{\rm ej} = 10 M_{\odot}$, distance $d = 50$ kpc, and hydrodynamic explosion energy $E_{\rm sn} = 1.5 \times 10^{51}$ erg [1,2].

Regarding the associated particle acceleration, only the forward SNR shock is considered. Its present high velocity $V_{\rm s}$ in excess of ≈ 5000 km s^{-1} suggests Bohm diffusion as the most reasonable approximation for the particle scattering characteristics. The effective magnetic field strength is taken to equal $B = (\rho/\rho_0) \times B_0$, where ρ_0 and ρ denote the upstream and the local gas mass density, respectively.

$$B_0 = \sqrt{2\pi \times 10^{-2} \rho_0 V_{\rm s}^2}$$

is an empirical measure of the magnetic field strength far upstream in the shock precursor, assumed to be amplified by the accelerating nuclear particles. This value of B_0 is about the same for all the thoroughly studied young SNRs up to now [10]. For the following it is assumed that this proportionality of the magnetic pressure $B_0^2/(8\pi)$ to the shock ram pressure $\rho_0 V_{\rm s}(t)^2$ also holds for an individual source like SN 1987A during its early temporal evolution, where the shock velocity $V_{\rm s}(t)$ is a function of the source age. It turns out that the resulting contemporary downstream magnetic field strength $B_{\rm d} \approx 20$ mG is indeed required to reproduce the observed radio and X-ray spectra.

3 Results

The gas dynamic equations and the transport equations for the accelerated nuclei and electrons are nonlinearly coupled by the CR backreaction on the gas as well as by gas heating through wave dissipation [2].

The gas dynamic quantitites plus B_0 are shown in figure 1.

The simultaneous solution of the energetic particle transport gives also the radio spectral index of the electron synchrotron radiation. Comparing the spatially integrated theoretical spectrum with the spatially integrated radio observations, that show an index of ≈ 0.9, determines the degree of nonlinear shock modification and thus the injection rate η of the nuclear particles as well as the electron:proton ratio $K_{\rm ep}(t)$. This is shown in figure 2. It turns out that the required high proton injection rate $\eta \approx 10^{-3}$ leads to a significant nonlinear modification of the shock: the total shock compression ratio $\sigma = 5.4 - 6$ is essentially larger, and the subshock compression ratio $\sigma_{\rm s} \approx 2.8 - 3.6$ is lower than the classical value of 4 for a pure gas shock.

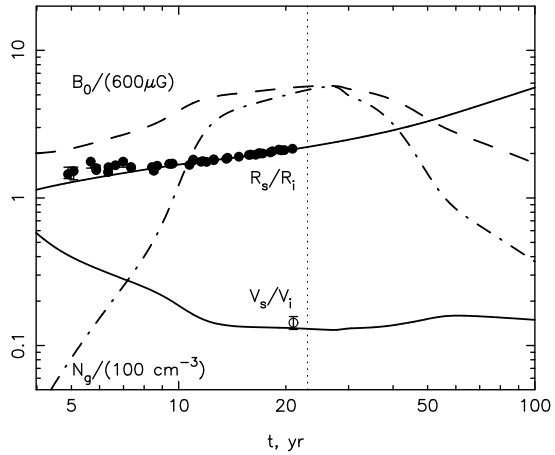

Figure 1: Shock radius $R_{\rm s}$ (solid), shock speed $V_{\rm s}$ (solid), gas density $N_{\rm g}$ (dash-dotted) and upstream magnetic field strength B_0 (dashed) at the current shock position, calculated as a function of time since SN explosion for $R_{\rm R} = 7 \times 10^{17}$ cm. The dotted vertical line marks the current epoch. The observed radius and the speed of the SN shock, as determined by radio observations [12], are shown as well. The scaling values are $R_{\rm i} = 3.1 \times 10^{17}$ cm and $V_{\rm i} = 28000$ km s^{-1}

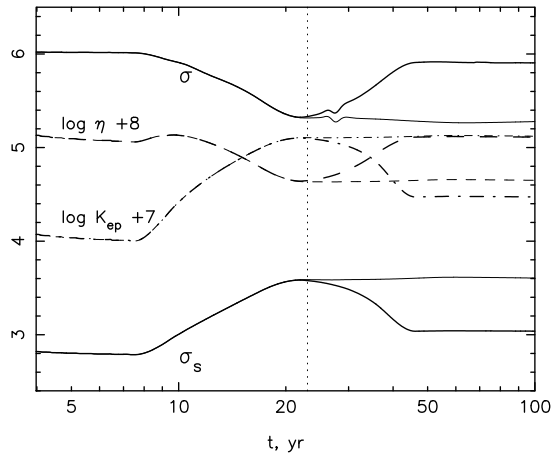

Figure 2: Shock compression ratio σ (solid), subshock compression ratio $\sigma_{\rm s}$ (solid), proton injection rate η (dashed), and electron-to-proton ratio $K_{\rm ep}$ (dash-dotted) as functions of time. The dotted vertical line again marks the current epoch. The thick and the thin lines here and in the subsequent figures correspond to an increasing and to a constant proton injection rate after an age of ~ 23 yrs, respectively

Figure 2 also indicates that the proton injection rate η changes during the SNR evolution, so that it has a minimum at an age of about 20 yr. This is required in order to fit the observed radio emission spectra [6] which are becom-

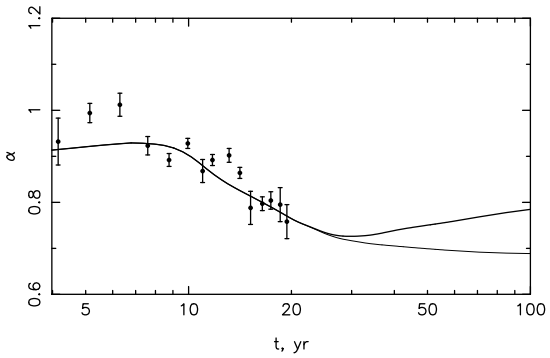

Figure 3: Spectral index of the spatially integrated radio synchrotron emission of SN 1987A as a function of time, together with the ATCA data [6]. The thick line corresponds to a recovery of the injection rate η to the value before the age of about 10 yr. Thin line: continued depression of η for ages > 23 yr

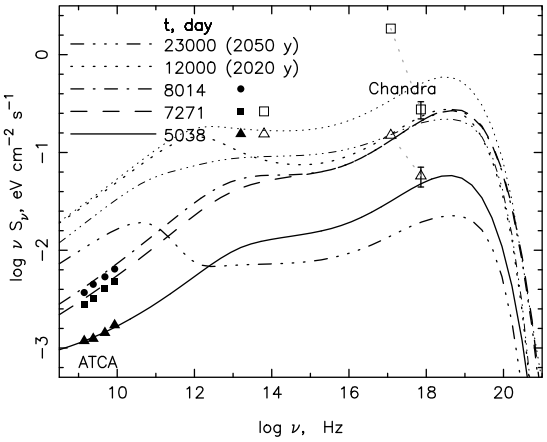

Figure 4: Spatially integrated synchrotron spectral energy density of SN 1987A, calculated for the five evolutionary epochs (solid curves). The ATCA radio data for three epochs [6] are shown as well, together with *Chandra* X-ray [5] data for two epochs (both, in the soft energy range at $\nu = 10^{17}$ Hz and, connected by dotted lines, in the hard energy range at $\nu = 6 \times 10^{17}$ Hz). The thin curves correspond to a continuing depression of the nuclear injection rate η after 23 yr

ing somewhat harder with time than a spectrum calculated with an unchanged injection rate - at least up to the present time (see figure 3). During the period from $t \approx 13$ yr to $t \approx 30$ yr, i.e. beyond the present epoch of radio observations, the shock is within the dense shell that corresponds to the observed equatorial ring. In this spatial region the magnetic field is expected to have an enhanced tangential component which should depress the nuclear injection rate [11].

Thereafter the injection rate is a priori unknown. It may increase again to the same level $\eta(t) \approx 10^{-3}$. This is one of the possibilities indicated in figure 2 and is calculated below. However, since the magnetic field vector in the free RSG wind is dominated by a component tangential to the SNR shock, also the possibility of a continuing depressed injection at a level similar to the value $\eta(t) \approx 4 \times 10^{-4}$ within the ring region is considered. The higher injection rate on the other hand yields, for $t > 23$ yr, a correspondingly larger shock modification, characterized by a larger shock compression ratio σ and a lower subshock compression ratio $\sigma_{\rm s}$ (figure 2).

The strong downstream magnetic field $B_d \approx 20$ mG leads to synchrotron cooling of the electrons with momenta $p > 10 m_{\rm p} c$. This makes the high energy part of the theoretically calculated form of the synchrotron spectrum ($\nu > 10^{13}$ Hz) very soft (see figure 4). At higher frequencies ($\nu = 10^{16} - 10^{19}$ Hz) the synchrotron spectrum becomes harder, possibly due to a pile-up effect. It hardens the spectrum of accelerated electrons, that undergo strong synchrotron losses, just near its exponential cutoff [13]. Under this condition the calculated synchrotron flux at frequency $\nu \approx 10^{17}$ Hz, which corresponds to a photon energy $\epsilon_\gamma = 0.5$ keV, is below the measured flux. This is a required condition because at energies $\epsilon_\gamma = 0.5 - 2$ keV the X-ray emission of SN 1987A is dominated by lines and is therefore mainly of thermal origin. At higher energies $\epsilon_\gamma > 3$ keV the X-rays are presumably of a predominant nonthermal origin. Therefore the fit of the measured X-ray flux for $\epsilon_\gamma = 3$ keV was used in the determination of the values of the 'injection parameters ($\eta(t)$ and $K_{\rm ep}(t)$) and of the amplified magnetic field $B_0(t)$ at the beginning of the shock precursor.

The soft (thermal) X-ray flux has, in fact, significantly flattened for the last ~ 1.5 yr (since day ~ 8000) [14]. This is roughly in agreement with the density distribution of figure 1, according to which the gas density $N_{\rm g}$ encountered by the shock is going through a maximum during the present period. The same should be true for the effective magnetic field strength B_0. The corresponding long-term prediction for the spatially integrated radio synchrotron flux is shown in figure 5. Presently the predicted light curve goes through a flat maximum, to secularly fall off with time thereafter in the RSG wind region.

The calculated spatially integrated gamma-ray spectral energy flux density (SED), shown in figure 6, is dominated by the π^0-decay component at all energies.

It is important to note here that the hadronic SED has nevertheless been renormalized by a factor $f_{\rm re} = 0.2$ compared to the amplitude resulting from the spherically symmetric model on which the entire calculation is predicated [11,2]. The reason for this a posteriori correction is the fact that the circumstellar environment is characterized by a Archimedean spiral topology, both in the BSG as well as in the RSG wind bubble environment. The corresponding uncertainty in the amplitude of the gamma-ray energy flux remains.

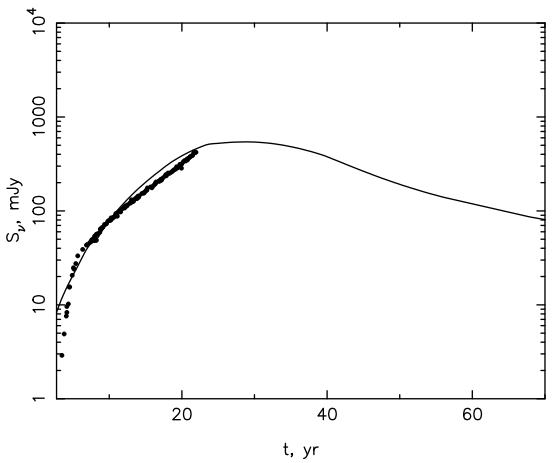

Figure 5: Calculated radio light curve for SN 1987A. The spatially integrated radio synchrotron data points are from the ATCA telescope at 1.4 GHZ [6]

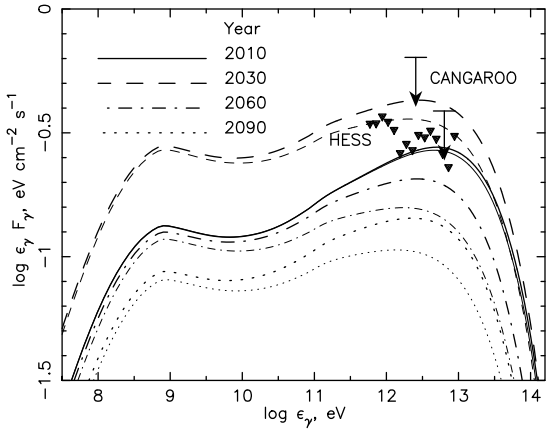

Figure 6: Spatially integrated gamma-ray energy flux from SN 1987A, calculated for four epochs (in *thin curves* for the future epochs also for a continuing small injection η rate, equal to the present one) The CANGAROO (arrows) [15] and the latest H.E.S.S. (triangles) [16] upper limits are shown as well

Since the SN shock is strongly modified, the gamma-ray spectrum at energies $\epsilon_\gamma > 0.1$ TeV is very hard: $F_\gamma \propto \epsilon_\gamma^{-0.8}$. At the current epoch the expected gamma-ray energy flux at TeV-energies is about $\epsilon_\gamma F_\gamma \approx 4 \times 10^{-13}$ erg cm^{-2} s^{-1}, and during the next 20 years it is expected to grow by a factor of about two with a subsequent temporal decrease $F_\gamma \propto R_{\rm s}^{-1}$ due to the rapid spatial decrease of the CSM density $\rho_{\rm w}(R_{\rm s}) \propto R_{\rm s}^{-2}$.

At present there exist only upper limits for the TeV emission. They have been obtained by the CANGAROO [15] and H.E.S.S. [16] instruments (figure 6). The latest H.E.S.S. upper limit is quite close to the SED estimated above. Even with the reservations formulated above, this is remarkable and justifies in the view of the present authors a deep observation of this object.

This work has been supported in part by the Russian Foundation for Basic Research (grant 10-02-00154), the Council of the President of the Russian Federation for Support of Leading Scientific Schools (project no. NSh-3526.2010.2), the Ministry of Education and Science (contract 02.740.11.0248). E.G. Berezhko acknowledges the hospitality of the Max-Planck-Institut für Kernphysik, where part of this work was carried out.

References

[1] McCray, R., ARA&A, 1993, **31**: 175-216
[2] Berezhko, E.G. Ksenofontov, L.T., Völk, H.J., ApJ, 2011, **732**: 58 (7pp)
[3] Berezhko, E.G., Ksenofontov, L.T., Astron. Lett., 2000, **26**: 639-656
[4] Berezhko, E.G., Ksenofontov, L.T., ApJ, 2006, **650**: L59-L62
[5] Park, S. et al.: 2007, AIP Conf. Proc. 937, Supernova 1987A: 20 Years After, ed. S. Immler et al., Melville, NY:AIP, p. 43-50
[6] Zanardo, G. et al., ApJ, 2010, **710**: 1515-1529
[7] Berezhko, E.G., Adv. Space Res., 2008, **41**: 429-441
[8] Potter, T.M. et al., ApJ, 2009, **705**: 261-271
[9] Chevalier, R.A., Dwarkadas, V.V., ApJ, 1995, **452**: L45-L48
[10] Völk, H.J., Berezhko, E.G., Ksenofontov, L.T., A&A, 2005, **433**: 229-240
[11] Völk, H.J., Berezhko, E.G., Ksenofontov, L.T., A&A, 2003, **409**: 563-571
[12] Ng, C.-Y. et al., ApJ, 2008, **684**: 481-497
[13] Drury, L.O'C. et al., A&A, 1999, **347**: 370-374
[14] Park, S. et al., to appear in ApJL, 2011; arXiv:1104.4825v1 [astro-ph.HE]
[15] Enomoto, R. et al., ApJ, 2007, **671**: 1939-1943
[16] Komin, N. et al., 2010, COSPAR Sci. Assembly (Bremen), E19-0096-10 (Poster, Nr. Thu-299)